The Journal of Experimental Biology 202, 2807–2818 (1999)
Printed in Great Britain © The Company of Biologists Limited 1999
JEB2106

MODELLING THE LOCOMOTOR ENERGETICS OF EXTINCT HOMINIDS

PATRICIA ANN KRAMER*

University of Washington, Departments of Anthropology and Orthopaedics, Seattle, WA 98104-2499, USA

*e-mail: pakramer@u.washington.edu

Accepted 20 July; published on WWW 30 September 1999

Summary

Bipedality is the defining characteristic of Hominidae and, as such, an understanding of the adaptive significance and functional implications of bipedality is imperative to any study of human evolution. Hominid bipedality is, presumably, a solution to some problem for the early hominids, one that has much to do with energy expenditure. Until recently, however, little attention could be focused on the quantifiable energetic aspects of bipedality as a unique locomotor form within Primates because of the inability to measure empirically the energy expenditure of non-modern hominids. A recently published method provides a way of circumventing the empirical measurement dilemma by calculating energy expenditure directly from anatomical variables and movement profiles.

Although the origins of bipedality remain clouded, two discernible forms of locomotor anatomy are present in the hominid fossil record: the australopithecine and modern configurations. The australopithecine form is best represented by AL 288-1, a partial skeleton of *Australopithecus afarensis*, and is characterized as having short legs and a wide pelvis. The modern form is represented by modern humans and has long legs and a narrow pelvis. Human walking is optimized to take advantage of the changing levels of potential and kinetic energy that occur as the body and limbs move through the stride cycle. Although this optimization minimizes energy expenditure, some energy is required to maintain motion. I quantify this energy by developing a dynamic model that uses kinematic equations to determine energy expenditure.

By representing both configurations with such a model, I can compare their rates of energy expenditure. I find that the australopithecine configuration uses less energy than that of a modern human. Despite arguments presented in the anthropological literature, the shortness of the legs of AL 288-1 provides no evidence that she was burdened with a compromised or transitional locomotor anatomy. Instead, she may well have been an effective biped at walking speeds, not despite her short legs, but rather because of them.

Key words: bipedality, human, locomotion, AL 288-1, *Australopithecus afarensis*, walking, energy expenditure.

Introduction

Bipedality is the defining characteristic of Hominidae and, consequently, the energetics of human bipedal locomotion has been of interest to anthropological researchers for many years. Scenarios of hominid evolution have been created to explain the rise of bipedality as predicated on such diverse factors as selection for energy efficiency (Foley, 1992), maximal thermal energy transfer (Wheeler, 1991a,b) and the use of display to maintain group cohesion (Jablonski and Chaplin, 1993). Without regard for which selective forces were at work, bipedality has been seen as a unitary adaptation, rather than as a general one with a variety of possible styles. Just as there are myriad forms of obligate and facultative quadrupedality, however, so too can there be different forms of bipedality. The style of bipedality that served the early hominids of the late Miocene was almost surely different from that of late Pliocene *Homo*.

The fossil record has begun to reveal that hominids can possess at least two body configurations (Jungers, 1991): relatively short-legged and long-legged versions. The former is characteristic of the early hominids, the australopithecines, while the latter is limited to *Homo*. Australopithecines are frequently seen as a transitional group, not fully modern in their form of bipedality and, consequently, energetically inefficient. Despite warnings from a few biomechanists (Witte et al., 1991), anthropologists have often equated short legs with inefficiency [an inherent bias of Steudel (1994), Webb (1996), Jungers (1982, 1991) and McHenry (1991b), to name a few]. The implicit logic is that short legs imply short stride lengths and that short strides require a higher cadence to maintain a particular velocity (Jungers, 1991). Unfortunately for anthropological analyses that rely on this logic, energetic expenditure is not solely a matter of the number of strides taken, but also of the energy required to take a single stride. This latter variable is dependent on the configuration of the locomotor anatomy, and shorter limb length implies, among other things, a smaller mass moment of inertia, which decreases energy expenditure. Consequently, it is reasonable to question the assumption that the short-legged

australopithecines were inefficient simply because they possessed short lower limbs.

Two methods have been employed in the biomechanical and physiological literature to evaluate locomotor energetics: (1) empirical methods that measure the volumetric rate of oxygen usage (submaximal $\dot{V}_{O_2}$) through the use of treadmills and oxygen analyzers, and (2) methods that combine theory with empirical data. The first method gives total treadmill metabolic rate (*TMR*), which is the sum of the physiological power required to sustain life (basal metabolic rate, *BMR*), the physiological power required to stand and maintain balance and control ($\dot{W}_{std}$), and the mechanical power required to move the whole body ($\dot{W}_{tot}$) at a level of mechanical efficiency (η):

$$TMR = BMR + \dot{W}_{std} + \frac{\dot{W}_{tot}}{\eta} . \quad (1)$$

BMR is reasonably well characterized for mammals, and Leonard and Robertson (1992) conclude that resting metabolic rate (the physiological power required to maintain bodily function while resting quietly) of hominoids does not deviate from the mammalian norm. The power required to stand and to maintain balance and control is less well characterized (Cavagna and Kaneko, 1977; Williams, 1985). In addition, mechanical efficiencies depend on the system delivering the power and remain difficult to quantify in complex living systems (Williams, 1985). The power delivery system of hominids can, however, be assumed to be cognate, and $\dot{W}_{std}$ and mechanical efficiencies should, therefore, be similar among hominids. A principal source of difference in the power required by hominids to locomote may derive from the different power required to move their differently configured bodies. Evaluating $\dot{W}_{tot}$ is, therefore, one important objective of this method, but its evaluation is limited by the necessity of having access to *TMR* for the (extinct) species in question.

The second method calculates $\dot{W}_{tot}$ directly from basic anatomical variables and quantified movement data. Over a given temporal interval, $\dot{W}_{tot}$ can be divided into two components, internal work (W_{int}) and external work (W_{ext}). W_{int} is the mechanical energy required to move the body elements relative to the center of mass of the whole body (Cavagna and Kaneko, 1977). Anatomical variables such as body segment lengths and mass moments of inertia are combined with movement data obtained from cinegraphic analysis and used to solve for internal energy. W_{ext} is the mechanical energy required to move the center of mass of the whole body relative to the ground and can be directly determined from force-plate analysis (Cavagna et al., 1976). One important problem with the second method is determining the percentage energy transfer among the elements of a limb and between the limbs and the torso (Cavagna and Kaneko, 1977). Willems et al. (1995) provide specific guidance for solving this problem. In addition, this method is limited in that it can only calculate the mechanical power required by a system ($\dot{W}_{tot}$) and not its metabolic rate or mechanical efficiency.

To understand the energetics of locomotion in modern humans, either or both methods are appropriate. To evaluate the energetics of extinct bipeds, however, the use of the first method is fraught with many problems. Obviously, the extinct hominid is not available to provide direct evidence, so a comparative approach is often used (see, for example, Rodman and McHenry, 1980). Predictive equations developed from the *TMR* of modern humans, chimpanzees (*Pan troglodytes*) and other non-human primates are used to predict the *TMR* of extinct hominids. This approach is flawed in that early hominids are neither habitual quadrupeds, as most other non-human primates are, nor do they exhibit the same body configuration as modern humans. The first method is, then, inappropriate for use in predicting the rate of locomotor energy expenditure of extinct hominids.

The second method holds much more promise. Since anatomical variables can be ascertained from the fossil record and the bipedal motion of australopithecines can be assumed to be similar to that of modern humans, the method of Willems et al. (1995) can be profitably used to develop a model that predicts the mechanical power requirements of extinct hominids. A corresponding model can also be developed of a modern human configuration and a comparison made between the two. This report details such an exercise.

Materials and methods

The model

The body is modeled as a series of rigid links representing the main components of the locomotor anatomy: foot, calf, thigh and pelvis. Segment masses are lumped at the centroid of each link, while the mass representing the head, arms and trunk (HAT) is lumped at the centerline of the pelvis. Fig. 1 is a sketch of the model. The left side is a mirror image of the right. Similar to equation 6 in Willems et al. (1995, p. 380), the total instantaneous energy of the whole body is defined as the sum of the kinetic and potential energies of the HAT and lower limbs:

$$E = \sum [m\boldsymbol{g}h + 0.5(mv^2 + I\omega^2)] , \quad (2)$$

where E is energy, m is mass, $\boldsymbol{g}$ is the acceleration due to gravity, h is segment length, v is translational velocity, I is moment of inertia and ω is angular velocity. The instantaneous energy of each link is computed in a similar manner (see below for discussion).

Two configurations of the model are established, one to represent a composite modern human female and the other to represent an extinct hominid, namely a member of *Australopithecus afarensis*. The modern configuration is developed from anthropometric data derived from Euro-American women (NASA, 1978). AL 288-1, also known popularly as ‘Lucy’, is chosen as the extinct hominid because she is the most complete hominid known from more than 2 million years ago. Over 40 % of her skeleton is known, including her pelvis, femur and tibia (Johanson et al., 1982). In addition, much debate in the anthropological literature has

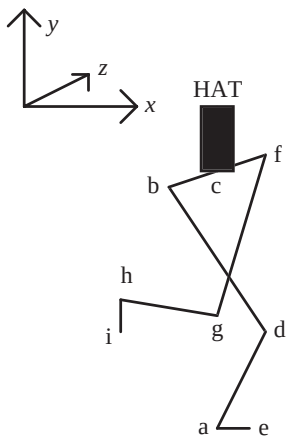

Fig. 1. Sketch of the model indicating joints and segments. The positive *x* axis points forward; the *y* axis points cephalid; the *z* axis points to the left. HAT, head, arm and trunk. Joints: e/i, ball of foot; a/h, ankle; d/g, knee; b/f, acetabulum; c, center of pelvis. Links: ae/hi, foot; ad/gh, calf; db/fg, thigh; bc/cf, half of pelvis.

centered on her energetic efficiency at bipedality or lack thereof.

Required inputs to the model

Detailed development of segment variables

Three anatomical variables are necessary to calculate the energy used in motion: segment lengths, segment masses and segment mass moments of inertia. The lengths that represent body segments in the australopithecine configuration are derived from AL 288-1, while those for the composite woman are an average of the adult female data presented in NASA (1978). The long bone lengths are combined with factors given in NASA (1978; Table 3) to determine the length of thigh and calf segments. These factors convert bone lengths into biomechanical lengths, taking into consideration the thickness of cartilage as well as the potential offset between anatomical landmarks and joint centerlines. The total pelvic width is determined by adding the femoral neck length of each side to the interacetabular distance. The length of segment bc/cf (see Fig. 1) is half the pelvic width. The length of the foot is the distance from the ball of the foot to the intersection of the tibia with the foot. Table 1 summarizes the segment (biomechanical) lengths.

Segment masses are determined for modern humans from the literature (NASA, 1978; Zihlman, 1984) and are derived mainly from cadaver dissections. Segment masses are much more problematic to develop for AL 288-1. Since average segment masses do exist for modern humans, I develop segment masses for AL 288-1 by factoring the modern segment mass by the ratio of total body masses. In other words, I assume that the same percentage of body mass is contained in each segment for both configurations. This assumption allows the comparison of the two configurations to be based solely on differences in segment length. Future analysis will address the effect of varying relative segment mass on the comparison. The mass of each limb segment is lumped at its centroid, while the mass of the head, arms and trunk (HAT) is lumped at the center of the pelvis (point c in Fig. 1). Table 1 shows the masses used for each segment and the percentage of body mass that each represents.

The final segment variables that are needed are the mass moments of inertia (*I*) of the segments. *I* for each of the limb segments is calculated using the regression formulae in NASA (1978; section IV, methods 2 and 3) that use total body mass and segment mass to approximate segment mass moment of inertia. Using this approach to develop *I* for the limb segments of AL 288-1 assumes that, although her limb length is different, the distribution of her musculature and other tissues is similar to that of modern humans. Table 1 gives the relevant values for both configurations.

The calculation of the mass moments of inertia for the HAT is more complicated because no simple method exists in the literature, although whole-body moments of inertia do exist. Consequently, an approximation based on the definition of mass moment of inertia must be used. If the HAT were allowed to rotate in three planes and was asymmetric in each, six total mass moments of inertia would be required. Fortunately, only three moments of inertia are needed: one for rotation in the *xz* (horizontal) plane, one for rotation in the *yz* (frontal) plane and

Table 1. *Segment variables for a modern woman and the extinct hominid AL 288-1*

	Modern woman				AL 288-1			
Segment	Length (m)	Mass (kg)	Relative mass (%)	*I* (kg m^2)	Length (m)	Mass (kg)	Relative mass (%)	*I* (kg m^2)
ae/hi (foot)	0.110	0.84	1.4	0.003	0.080	0.46	1.4	0.003
ad/gh (calf)	0.390	3.00	5.0	0.035	0.265	1.65	5.0	0.019
db/fg (thigh)	0.373	6.00	10.0	0.110	0.252	3.30	10.0	0.053
bc/cf (HAT_{xx})	0.130	40.32	67.2	8.9	0.105	22.18	67.2	2.34
(HAT_{yy})				0.43				0.18
(HAT_{xy})				0.95				0.43

See Fig. 1 for definition of segments.
I is mass moment of inertia; $_{xx}$, $_{yy}$, $_{xy}$ indicate the mass moments of inertia calculated about the *x* axis, *y* axis and *xy* plane, respectively.

a cross-product term. The terms for the *xz* and *yz* planes (I_{bcyy} and I_{bcxx}) are needed because the HAT rotates in both, i.e. an angular velocity of the HAT exists in each plane. The cross-product term (I_{bcxy}) is necessary because the body is not symmetrical about the *z* axis. Integral formulae exist to calculate *I*; however, they require that an equation that describes the shape of the object be available which, in this case, it is not. An approximation of the integral can be determined, however, by dividing the HAT into small (pseudo-differential) elements. This approximation then allows the mass moments of inertia to be calculated *via* the summations (Meriam, 1978):

$$I_{bcxx} = \sum (y^2 + z^2)\mathrm{d}m\,, \tag{3}$$

$$I_{bcyy} = \sum (x^2 + z^2)\mathrm{d}m\,, \tag{4}$$

$$I_{bcxy} = \sum xy\mathrm{d}m\,. \tag{5}$$

The mass of each element (d*m*) and distance from the centroid in each axis (*x*, *y* and *z*) is calculated. The contribution of each block is then summed over the complete HAT. I use this technique and demonstrate its use below for I_{bcyy}.

Fig. 2 shows an idealized view looking down on the HAT. Fig. 2A shows the distance of each block from the *x* axis, while Fig. 2B shows the distance from the *z* axis. The distances shown in Fig. 2A,B are relative, or unfactored, to allow the same values to be used for any configuration. The mass of each block is shown in Fig. 2C,D for the composite woman and AL 288-1, respectively. AL 288-1 has smaller values because, although she was approximately the same width (in the frontal plane) as a modern woman, she was shorter and narrower and, consequently, weighed less.

The contribution to the HAT mass moment of inertia represented by each differential element is obtained by adding the square of the distances shown in Fig. 2A,B and multiplying by the differential mass shown in Fig. 2C,D. The result of this calculation is shown in Fig. 2E,F for the composite woman and AL 288-1, respectively. The total mass moment of inertia is the sum of the individual blocks. This technique is used to develop the other two moments of inertia (I_{bcxx} and I_{bcxy}). All mass moments of inertia are shown in Table 1.

I performed a check of this technique by calculating the HAT mass moments of inertia of the six male subjects shown in Chandler et al. (1975). Chandler et al. (1975) provide the mass and centroid location of each body segment (head, torso, right and left upper arm, lower arm and hand) included in the HAT. I was able, therefore, to transfer the axis of rotation from the center of mass of each segment to the center of the pelvis through the application of the parallel axis theorem (Meriam, 1978). Although the data of Chandler et al. (1975) cannot be used to estimate population parameters, they are sufficient to give a general guideline because my composite woman is of similar body mass (60 kg *versus* 50.62–89.15 kg, respectively) and stature (160.4 cm *versus* 164.5–181.7 cm, respectively) to Chandler's subjects. I calculate I_{bcxx} for Chandler's subjects to be 7–14 kg m^2 and I_{bcyy} to be 0.4–1 kg m^2. The method I present above yields similar values (see Table 1). I did not use the data presented in Chandler et al. (1975) to calculate the mass moments of inertia used in this analysis because they are

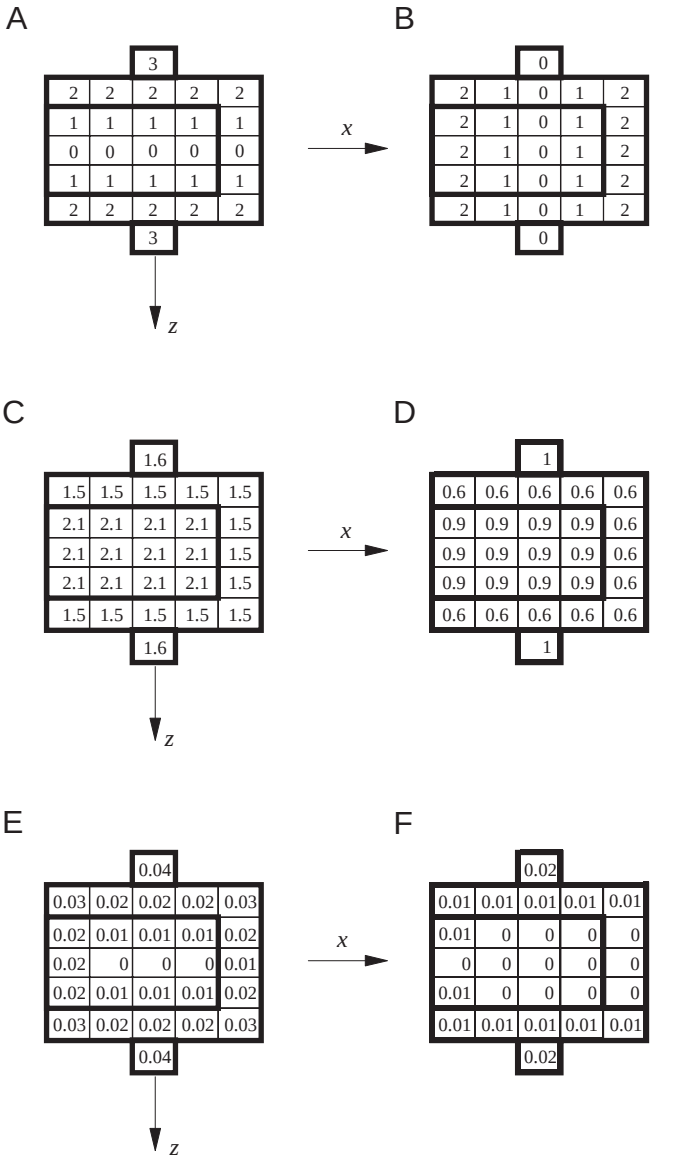

Fig. 2. Relative distance from the *x* and *z* axes, mass (kg) and mass moment of inertia (kg m$^{2)}$ for a composite woman and AL 288-1. (A) Relative distance from the *x* axis for each block. (B) Relative distance from the *z* axis for each block. (C) Mass of each block in the modern configuration. (D) Mass of each block in the configuration of AL 288-1. (E) Contribution of each block to the total mass moment of inertia about the *y* axis (I_{bcyy}) of the composite woman. (F) Contribution of each block to the total mass moment of inertia about the *y* axis (I_{bcyy}) of AL 288-1. The figure shows an idealized view looking down on the head, arms and trunk (HAT). Note that these figures are schematic and are not drawn to scale. The large rectangular outline represents the trunk, the smaller interior rectangle the head, and the two small exterior rectangles the arms. The *x* axis divides the body into symmetrical left and right sides, while the *z* axis divides the body into anterior and posterior portions. Each rectangle is divided into a number of blocks. The centroid is assumed to be located at the geometric center of the body rectangle.

inappropriate for use in developing the HAT mass moments of inertia for AL 288-1, whose mass and stature are well outside the range of Chandler's subjects.

Movement profiles

In addition to the three segment variables described above, movement profiles are needed to solve the energy equations. By 'movement profile', I mean the variation in the angles between the links (θ_{ad}, θ_{db}, etc.) with the percentage of the stride cycle. These angular excursions, in combination with segment lengths, are used to determine translational (v) and rotational (ω) velocity. Angular excursions are available in the literature (Perry, 1992; Winter, 1987; Inman et al., 1981) for modern humans walking at various velocities. I construct an 'average' woman from these. Because no movement profiles are known for australopithecines, I use the same profiles for both configurations.

To develop the joint angular excursions, I used the average hip, knee and ankle angles given by Winter (1987) for slow, natural and fast cadences and combined them with the angles for pelvic swing (θ_{bcxz}) and pelvic tilt (θ_{bcyz}) from Inman et al. (1981). Winter defines a 'slow' cadence as approximately $1\,m\,s^{-1}$, while a 'natural' cadence is $1.36\,m\,s^{-1}$ and a 'fast' cadence is $2\,m\,s^{-1}$. Modern humans tend to change from a walk to a run between 2 and $2.4\,m\,s^{-1}$ (Waters et al., 1988). Winter's 'fast cadence' is, therefore, close to the fastest (normal) walk exhibited by modern adults. One cautionary note should be added here: this definition of cadence assumes an average leg length that might be found in someone 1.65–1.85 m tall. Shorter people with shorter legs might feel that $1.36\,m\,s^{-1}$ was a 'fast' rather than a 'natural' walk. The concept of equivalent velocity, as discussed below, attempts to compensate for the effect of leg length on locomotor effort.

I use the angular excursions found in Winter (1987) rather than other published sources because Winter's data are clearly detailed. Unfortunately, other researchers, including Inman et al. (1991), present data that, although more elaborate, are not as easily understood. In addition, Inman et al. (1991) presents curves for individuals without providing any estimates of basic anthropometrics or a method to create an average person from the individuals. Winter (1987; Table 32) provides joint angles at 2° increments of the percentage of the stride cycle and standard deviations.

The angular excursions of the lower limb (θ_{ae}, θ_{ad} and θ_{db}) are created from the angles presented in Winter (1987). These angular excursions are shown in Fig. 3A,B,C, respectively. Pelvic swing (θ_{bcxz}) (Fig. 3D) and pelvic tilt (θ_{bcyz}) (Fig. 3E) are developed from Inman et al. (1991).

Equivalent velocity

Because the configurations of the composite woman and AL 288-1 differ substantially in stature and leg length, a velocity that a modern human perceives as slow might be a fast walk for a biped such as AL 288-1. To compare the two configurations on an equitable basis, velocities that represent equivalent effort are needed. 'Effort' could involve any physiological or psychological process that influences movement. Alexander (1984) presents a method that can be used to calculate an equivalent velocity for one configuration given the velocity and a characteristic length of another. In this case, leg length is used. Two dimensionless parameters are created, one of which is the Froude number while the other relates stride length and stature. They are assumed to be related to each other *via* some function (f):

$$SL/ST = f[u/(\boldsymbol{g}l)^{0.5}] \quad (6)$$

or

$$f^{-1}(SL/ST) = u/(\boldsymbol{g}l)^{0.5}, \quad (7)$$

where SL is stride length, ST is stature, u is horizontal translational velocity and l is leg length. If the two configurations are equivalent, then:

$$f^{-1}(SL/ST)_{mod} = f^{-1}(SL/ST)_{AL288} \quad (8)$$

and

$$u_{AL288} = u_{mod}\sqrt{l_{AL288}/l_{mod}}. \quad (9)$$

The velocities that are related by equation 9 are considered to be 'equivalent' and are given the designation slow, natural and fast in keeping with Winter (1987).

Model calculations

Development of angular velocities (ω)

Once the angular excursions are defined, then the angular velocities can be calculated. Because the angular excursions form a continuous curve, the derivative is the instantaneous slope, i.e. the tangent, of the curve at any point in time. If you allow the temporal increment to get larger, then the derivative is simply the slope of a line between two successive angles divided by the difference in time between the two. I calculate angular velocity in this way. In addition, I average angular velocity over three successive temporal increments to produce a smooth angular velocity curve. This procedure is similar to that of Willems et al. (1995). Fig. 4 shows the final angular velocity profiles for each angle and equivalent velocity.

Displacement of a point

When the movement profiles have been developed, the displacement of each joint in the model can be calculated. The displacement of each point is determined by idealizing the model as an open kinematic loop. From 0 to 40 % of the stride cycle, point a (see Fig. 1) is in contact with the ground and the displacement of all other points can be determined sequentially with reference to point a. From 40 to 50 % of the stride cycle, point e is the point of contact and reference.

Calculation of the velocity of each point

The displacements are used to calculate the translational velocity of each point for each temporal increment. Total time to complete a step can be calculated from the total distance moved during a step and the average velocity of the HAT. Total distance moved is simply the difference in x axis displacement of point c from t=0 % of the stride cycle to t=50 % of the stride cycle. Instantaneous velocity is calculated

as the difference in the position of a point between two temporal increments divided by the duration of the increment.

Mechanical energy

Equation 2 gives the total energy of the body, but more useful for the present analysis is the energy of each leg and the HAT. If the right and left legs and the pelvis are treated separately, the following equations are obtained:

$$E_{p,pe} = m\boldsymbol{g}(dy_c), \quad (10)$$

$$E_{p,r} = m_{db}\boldsymbol{g}(dy_d + dy_b)/2 + m_{ad}\boldsymbol{g}(dy_a + dy_d)/2 + m_{ae}\boldsymbol{g}(dy_a + dy_e)/2, \quad (11)$$

$$E_{p,l} = m_{db}\boldsymbol{g}(dy_f + dy_g)/2 + m_{ad}\boldsymbol{g}(dy_h + dy_g)/2 + m_{ae}\boldsymbol{g}(dy_h + dy_i)/2, \quad (12)$$

$$E_{k,r} = 0.5\{[m_{ad}v_{ad,c}^2 + I_{ad}(\omega_{ad})^2] + [m_{ae}v_{ae,c}^2 + I_{ae}(\omega_{ae})^2] + [m_{db}v_{db,c}^2 + I_{db}(\omega_{db})^2]\}, \quad (13)$$

$$E_{k,l} = 0.5\{[m_{ad}v_{gh,c}^2 + I_{ad}(\omega_{gh})^2] + [m_{ae}v_{hi,c}^2 + I_{ae}(\omega_{hi})^2] + [m_{db}v_{fg,c}^2 + I_{db}(\omega_{fg})^2]\}, \quad (14)$$

and

$$E_{k,pe} = 0.5mv_c^2 + 0.5(I_{bcyy}\omega_{bcxz}^2 + I_{bcxx}\omega_{bcyz}^2) - I_{bcxy}\omega_{bcxz}\omega_{bcyz}, \quad (15)$$

where dy is the position along the y axis.

Once the potential (E_p) and kinetic (E_k) energies have been determined for the right and left legs and the pelvis for each temporal increment, then the change in energy between two increments can be determined and summed. This change, dE, is simply the difference between two consecutive temporal increments. In the following discussion, the equations for the left leg are shown while those for the right leg and pelvis are similar:

$$dE_{p,l,i} = E_{p,l,i} - E_{p,l,i-1}, \quad (16)$$

$$dE_{k,l,i} = E_{k,l,i} - E_{k,l,i-1}, \quad (17)$$

$$dE_{tot,l,i} = E_{p,l,i} - E_{k,l,i}. \quad (18)$$

A positive value of d$E_{tot,i}$ indicates that energy was added to the system, while a negative value of d$E_{tot,i}$ indicates that there was surplus energy. Changes in energy (E_{sum}) are summed for the right leg, left leg and pelvis. Since the energy of interest is that which must be added to the system to keep it moving, only a positive d$E_{tot,i}$ is added to E_{sum}:

$$E_{sum,l} = \sum dE_{tot,l}, \quad (19)$$

when

$$dE_{tot,l} > 0.$$

No storage mechanism exists in this model. Surplus energy is, therefore, assumed to be dissipated through some unspecified method. The mechanism through which energy is

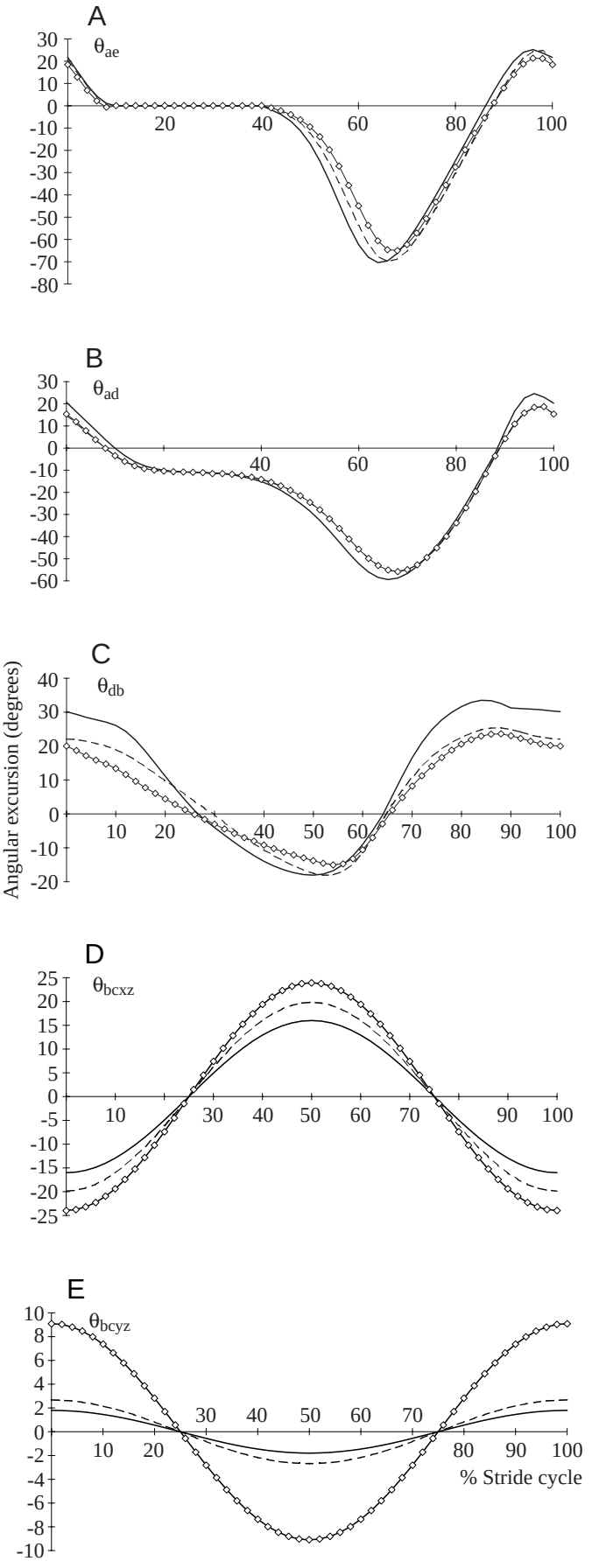

Fig. 3. Angular excursion (degrees) *versus* percentage of the stride cycle at three walking velocities. (A) Right foot, θ_{ae}; (B) right calf, θ_{ad}; (C) right thigh, θ_{db}; (D) pelvic swing, θ_{bcxz}; (E) pelvic tilt, θ_{bcyz}. Fast equivalent velocity is shown with a solid line. Natural equivalent velocity is shown with a dashed line. Slow equivalent velocity is shown with diamonds.

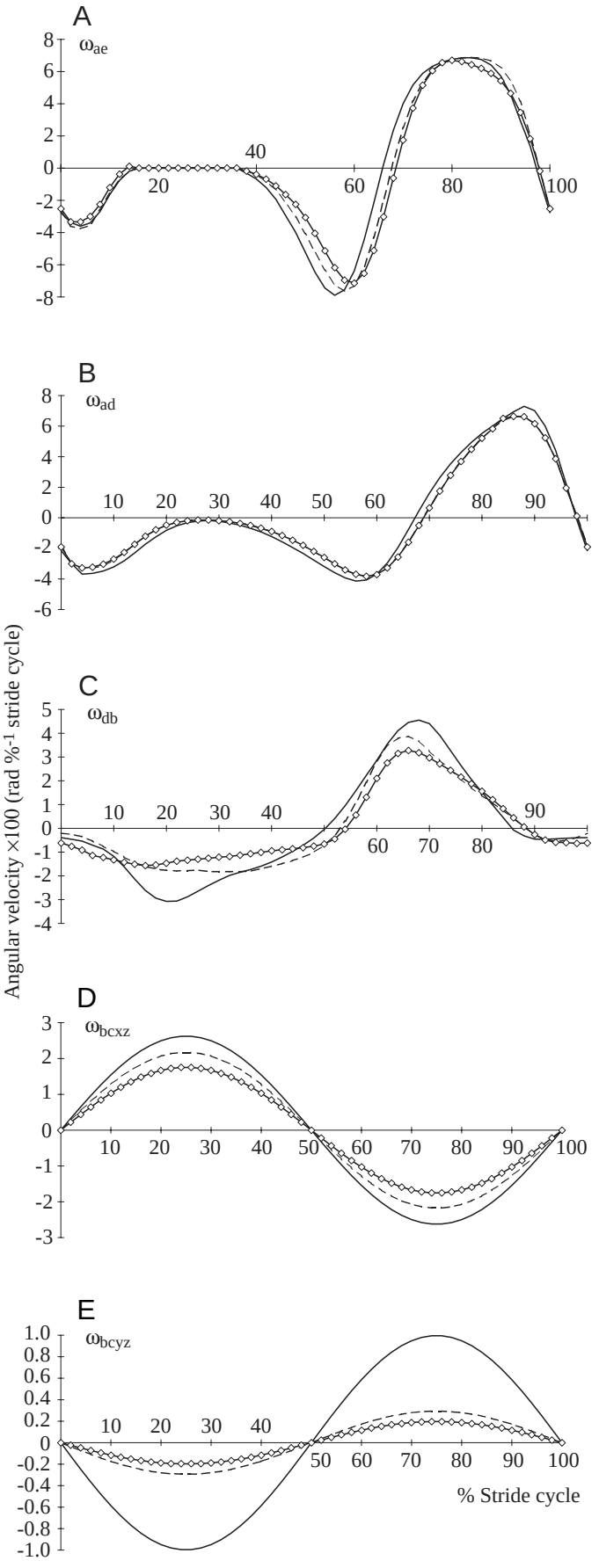

Fig. 4. Angular velocity (rad %$^{-1}$ stride cycle) *versus* percentage of the stride cycle. (A) Right foot, ω_{ae}; (B) right calf, ω_{ad}; (C) right thigh, ω_{db}; (D) pelvic swing, ω_{bcxz}; (E) pelvic tilt, ω_{bcyz}. Fast angular velocity is shown with a solid line. Natural angular velocity is shown with a dashed line. Slow angular velocity is shown with diamonds.

added to the system is also unspecified because the model is designed to determine how much energy is added, not in what manner this addition is accomplished.

The mass-specific mechanical power ($\dot{E}_{sum}$) is calculated using $E_{sum,l}$, the total body mass of each configuration (m) and the time to required to take a step (t_{max}):

$$\dot{E}_{sum,l} = \frac{E_{sum,l}}{m t_{max}}, \quad (20)$$

$$\dot{E}_{sum,rl} = E_{sum,l} + E_{sum,r}, \quad (21)$$

$$\dot{E}_{tot} = \dot{E}_{sum,rl} + \dot{E}_{sum,pe}. \quad (22)$$

Similarly, cost of transport (*CoT*), the mass-specific energy required by a configuration to move a given distance, is determined using $\dot{E}_{sum}$ and average forward velocity (v_f):

$$CoT_l = \frac{E_{sum,l}}{v_f}, \quad (23)$$

$$CoT_{rl} = CoT_l + CoT_r, \quad (24)$$

$$CoT_{tot} = CoT_{rl} + CoT_{pe}. \quad (25)$$

Results

Conformity of model to expectations

Displacement pattern

To be valid, the model should demonstrate several important features of walking, including: (1) no negative vertical displacements, i.e. below ground level, of the swing foot; (2) heel strike of the stance foot at t=0 % of the stride cycle and of the swing foot at t=50 % of the stride cycle; (3) heel-off for the stance leg before t=50 % of the stride cycle with the toe in contact with the ground; and (4) double stance (swing and stance feet in contact with the ground) from approximately t=0 % to t=10 % of the stride cycle. As shown in Table 2 and Fig. 5, the stance leg fulfills the expectations derived from empirical observations of human walking patterns. The swing leg also has remarkable success in meeting these expectations. Because the displaced location of the swing heel and toe is the sum of the displacements of the other segments and positional errors accumulate, it is expected that the swing foot would have more difficulty in attaining the correct position. For instance, in the australopithecine model, the maximum foot drag (negative vertical displacement) is caused by the heel and is –0.005 m. This represents an out-of-position error of less than 1 %. Both a visual inspection of the patterns and a quantitative evaluation indicate that the model predicts positions in space that are in fundamental agreement with empirical observations.

Table 2. *Displacement pattern*

Configuration	Equivalent velocity	Swing leg: Maximum foot drag (m)	Swing leg: Heel at *t*=50 % (m)	Stance leg: Heel at *t*=0 % (m)	Stance leg: Toe at *t*=0 % (m)	Stance leg: Heel at *t*=50 % (m)	Stance leg: Toe at *t*=50 % (m)	Stride length: Predicted[1] (m)	Stride length: Model[2] (m)	Double stance period (% stride)
Modern woman	Fast	–0.003	0	0	0.041	0.005	0	1.52	1.48	7
	Natural	0	0	0	0.038	0.023	0	1.31	1.22	10
	Slow	0	0	0	0.035	0.018	0	1.16	1.10	8
AL 288-1	Fast	–0.005	–0.004	0	0.030	0.023	0	1.09	1.03	7
	Natural	0	0	0	0.028	0.017	0	0.94	0.85	10
	Slow	0	0	0	0.025	0.013	0	0.83	0.77	8

Values for the swing and stance leg are the distance above the ground for each location at the indicated time.
Maximum foot drag is the minimum vertical position of either the toe or heel.
Negative values indicate positions that are below ground level.
Stride lengths are the horizontal distance between consecutive heel strikes of the same heel.
The double stance period is the percentage of time that both feet are in contact with the ground.
[1]Although Grieve and Gear (1966) speak of an 'adult walking pattern' with no differentiation between the pattern for males and females, their data (Table 1, p. 381) show that a significant difference exists. Using their data, I developed an equation, $SL = (0.873/ST)(v_f/ST)^{0.31}$, where SL is stride length, ST is stature and v_f is forward velocity, whose coefficients were determined only by the data for adult females in their study (N=9).
[2]Calculated from the model as twice the distance traveled by the center of the pelvis (point c; see Fig. 1).
t, time.

Stride length

Stride length can be calculated for a modern human from sex, velocity and stature (Grieve and Gear, 1966) and from the model as twice the horizontal displacement of the HAT (point c) from *t*=0 % to *t*=50 % of the stride cycle. Table 2 shows predictions from both methods of calculation of stride lengths for both configurations. The model predicts stride lengths for the modern configuration that are less than 7 % smaller than predicted. The calculated stride length for AL 288-1 of 0.77–1.03 m differs by as much as 11 % from the predictions. The short legs and consequent short stature of the australopithecine configuration, however, potentially place it beyond the valid range of the predictive equations. Stride lengths for AL 288-1 derived from the model are reasonable when compared with those seen in the Laetoli hominid footprint trail (Leakey, 1987; White, 1977, 1980), whose stride lengths range from 0.62 to 0.944 m (Alexander, 1984; Robbins, 1987; Tuttle, 1987).

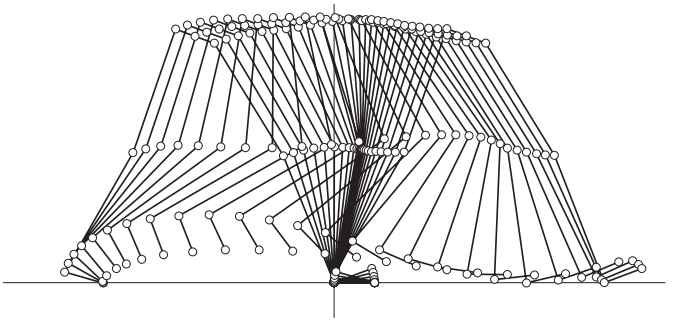

Fig. 5. Displacement of points in fast equivalent velocity for a modern human. Displaced points are calculated from segment variables and angular excursions and are shown in increments of 2 % of the stride cycle for one step (*t*=0 % to *t*=50 % of the stride cycle). The center vertical line indicates the location of zero *x* displacement. The horizontal line indicates the location of zero *y* displacement. *t*, time.

Horizontal velocity

The horizontal (*x* direction) velocity can be calculated from the variation in *x* displacement. The average velocity of the center of the pelvis (point c) over 50 % of the stride cycle should equal the velocity of forward progression of the body because point c will move half the stride length in 50 % of the stride cycle time. Other points in the model will not average to the forward progression velocity over 50 % of the stride cycle because they do not move half the stride length in half the stride cycle time. For instance, while the swing foot moves a distance equal to the stride length, the stance foot remains stationary. The average velocity of point c for both configurations and all equivalent velocities is equal to the input forward velocity (data not shown).

Energy required to walk

Comparison between the model and empirical data for modern humans

To determine whether the rate of energy consumption calculated by the model is similar to empirical observations of modern humans, I compare the model-generated data with empirical data from Cavagna and Kaneko (1977) and Cavagna et al. (1976). Cavagna and Kaneko (1977) calculate internal mechanical power, $\dot{W}_{int}$, as the sum of the changes in kinetic energy of both the arms and legs and present it as a function of forward velocity. Fig. 6 shows that $\dot{W}_{int}$ is lower than $\dot{E}_{sum}$ calculated in the present study. At slow and natural equivalent

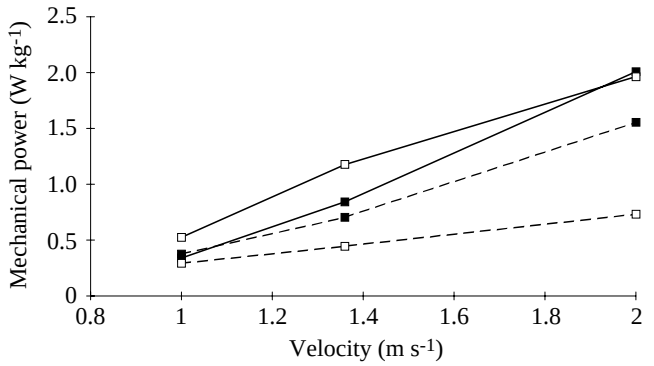

Fig. 6. Mass-specific mechanical power *versus* velocity for modern humans. Mass-specific mechanical power of the pelvis calculated using the present model, $\dot{E}_{sum.pe}$, is shown as a solid line with open squares; that of the right and left legs, $\dot{E}_{sum.rl}$, is shown as a solid line with filled squares. The mass-specific external power required to move the center of the mass of the whole body taken from Cavagna et al. (1976) ($\dot{W}_{ext}$) is shown as a dashed line with open squares; the mass-specific internal power from Cavagna and Kaneko (1976) ($\dot{W}_{int}$) is shown as a dashed line with filled squares.

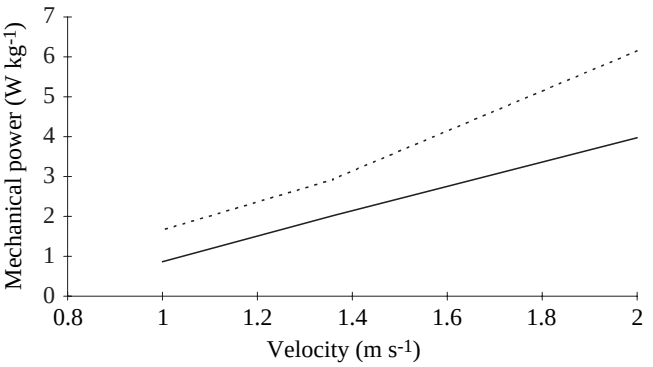

Fig. 7. Mass-specific mechanical and physiological power *versus* velocity. Mechanical power derived from the model ($\dot{E}_{tot}$) is shown as a solid line. Physiological power, calculated as treadmill metabolic rate (*TMR*) minus standing metabolic rate (*SMR*) and taken from data on humans (see text for details), is shown as a dotted line.

velocity, the values of Cavagna and Kaneko (1977) are similar to those from the model, while at the fast equivalent velocity, the model produces values higher than Cavagna and Kaneko observed. Possible causes for this discrepancy are as follows: (1) their values do not include the effect of changes in potential energy; and (2) their model does not include an element for the foot.

Cavagna et al. (1976) describe the total mechanical power changes of the center of mass of the body, $\dot{W}_{ext}$. Fig. 6 shows that their values of $\dot{W}_{ext}$ are smaller than $\dot{E}_{sum,pe}$ calculated in the present study. One possible explanation for this discrepancy is that $\dot{E}_{sum,pe}$ is calculated from the translational and rotational velocities of the center of the pelvis and not from the actual center of mass of the body. Waters et al. (1973) suggest that the variation in forward velocity of the torso increases from head to pelvis, and the difference in forward velocity between the center of mass of the HAT and the center of the pelvis may vary substantially. If the forward velocity of the pelvis varies through the stride cycle more than that of the center of mass of the body, then $\dot{E}_{sum,pe}$ should substantially exceed $\dot{W}_{ext}$.

As a final test of the model, I compare $\dot{E}_{tot}$ with a prediction of treadmill metabolic rate (*TMR*, from Pandolf et al., 1977) minus $BMR+\dot{W}_{std}$, which is a measure of standing metabolic rate (*SMR*). *SMR* is calculated from resting metabolic rate (established for Anthropoidea by Leonard and Robertson, 1992) and the metabolic cost of resting and standing for women (FAO/UNU/WHO, 1985; Annex 5). At all velocities, $\dot{E}_{tot}$ is less than the empirically determined values (Fig. 7). As equation 1 indicates, physiologically derived energy expenditures are influenced by both balance and control requirements and by the efficiency of the power delivery system, and neither of these parameters is known for the whole body at this time. $\dot{W}_{tot}$ must, therefore, be less than *TMR*–*SMR*, but exactly how much smaller is unknown. In addition, because of the differences between $\dot{E}_{sum,pe}$ and $\dot{W}_{ext}$ cited above, $\dot{E}_{tot}$ will be larger than $\dot{W}_{tot}$.

Comparison between modern human and AL 288-1

The mass-specific mechanical power required to move the lower limbs ($\dot{E}_{sum,rl}$) is shown in Fig. 8. The configuration that represents AL 288-1 requires less energy to move its limbs than does that of the composite woman when the two are compared over the same temporal increment and for the same mass. This finding holds true for all three equivalent velocities. The cost of transport (CoT_{rl}) is shown in Fig. 9. Interestingly, the configuration of AL 288-1 requires essentially the same energy (within 2 %) to move 1 kg of mass over 1 m as does that of the modern woman.

Discussion

On a mass-specific basis, the configuration developed from the fossil remains of AL 288-1 uses less energy to move than,

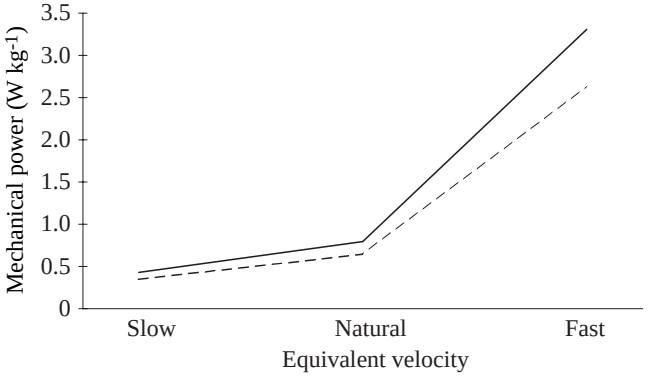

Fig. 8. Mass-specific mechanical power ($\dot{E}_{sum,rl}$) required to move the lower limbs for modern humans (solid line) and AL 288-1 (dashed line) *versus* equivalent velocity. $\dot{E}_{sum,rl}$ was calculated using the present model.

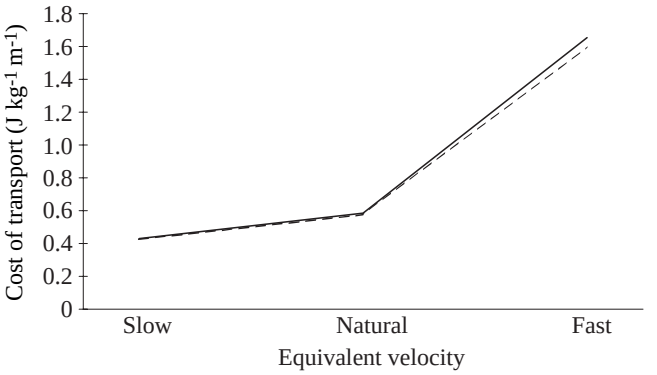

Fig. 9. The cost of transport of modern humans (solid line) and AL 288-1 (dashed line) *versus* equivalent velocity. The cost of transport was calculated using the present model.

and has the same cost of transport as, the modern human configuration. This deceptively simple finding has important ramifications for the understanding of AL 288-1 and her congeners. The idea that the individuals that composed *Australopithecus* in general, or *A. afarensis* specifically, were transitional bipeds – encumbered with short legs because of continued reliance on arboreal resources, but energetically compromised because of their shortness – appears no longer to be tenable. Short legs do not by themselves make a biped inefficient, as an understanding of the basic principles of dynamics indicates. Rather, 'designing' an efficient biped is a matter of balancing the conflicting effects of increasing equivalent velocity (and therefore energy expenditure) against decreasing internal and external work. While short legs can force an individual to take more steps, which does require more energy expenditure in one part of the system, short legs can also decrease the energy used per step.

Of course, the locomotor anatomy of Al 288-1 may have contained elements that would have decreased her efficiency at locomotion. She may have had a larger proportion of fast-twitch muscles, a less optimal arrangement of stabilization musculature or a host of other trade-offs that may have limited her proficiency. Unfortunately, the fossilized remains of osteological elements provide little insight into the soft tissue anatomy of extinct creatures. We will, therefore, probably never fully understand the mechanism by which australopithecines moved in their environment. Nonetheless, the central issue discussed here is that short legs are not sufficient evidence to claim that the form of bipedality exhibited by AL 288-1 was inefficient or transitional.

One important question that has not been addressed is whether it is appropriate to use movement profiles developed from modern humans for AL 288-1. An extensive, and often acrimonious, debate has flourished in the anthropological literature over whether the locomotor anatomy of AL 288-1 is 'modern' (Lovejoy et al., 1973; McHenry, 1975; White, 1980; Latimer et al., 1987; Lovejoy, 1988; Latimer and Lovejoy, 1989) or not (Robinson, 1972; Zihlman, 1978; Zihlman and Brunker, 1979; Jungers, 1982; Stern and Susman, 1983). With no general agreement in sight, I find no character in the locomotor anatomy of AL 288-1 that prohibits the motions that modern humans undergo and, instead, find many characters that indicate that AL 288-1 could move as modern humans do (Kramer, 1998). In addition, the Laetoli hominid footprint trail is remarkably human-like (Robbins, 1987; Tuttle, 1987) and, with a date of greater than 3.6 million years ago (Drake and Curtis, 1987), attributable to *Australopithecus*. While it seems almost certainly true that the motion of AL 288-1 was somewhat different from that of modern humans, it is equally likely that the motion of her limbs was fundamentally similar to that of modern humans. AL 288-1 could flex and extend her thighs, straighten her knees, swing and tilt her pelvis and push off with her feet just as modern humans do. Because of this, the use of the movement profiles developed from modern humans is justified (Kramer, 1998).

The method of Willems et al. (1995) is a useful technique for exploring the locomotor energetics of extinct hominids. Their method provides a procedure for predicting energetic expenditure in animals on whom experimentation is impossible. The model described herein, which was developed from their approach, accurately describes the motion of modern human bipeds and can be used profitably to evaluate the locomotor energetics of AL 288-1.

When the rates of energy expenditure of the two configurations are compared, several pivotal issues in paleoanthroplogy become clearer. The long legs of *Homo* are not the inevitable outcome of selection for efficient bipedality. Instead, the important anthropological questions of 'why bipedality?' and 'why long legs?' need to be as clearly separated in the minds of researchers as the origin of bipedality and the development of long legs were in geological time. The locomotor anatomy of AL 288-1 has often been misunderstood as a complex compromise between efficient ape arboreality and efficient (modern) bipedality. While her pelvis has been seen by most anthropologists as strong evidence of terrestrial bipedality, many have decried her short legs as explicable as useful only to a creature dependent on climbing as a fundamental adaptation. This analysis clearly indicates that AL 288-1 was not fundamentally compromised by her short legs and that short legs can be appropriate for a terrestrial biped. AL 288-1 may well have been an effective biped at walking speeds, not despite her short legs, but rather because of them.

List of abbreviations

BMR	basal metabolic rate ($W\,kg^{-1}$)
CoT	cost of transport ($J\,kg^{-1}\,m^{-1}$)
d*E*	difference in energy between two consecutive temporal increments (J)
d*m*	pseudo-differential mass of a block (kg)
d*x*	*x* axis displacement of a point (m)
d*y*	*y* axis displacement of a point (m)
E	energy (J)
$\dot{E}$	energy expenditure per unit of time (power) calculated in the present study ($W\,kg^{-1}$)
f	function

$\boldsymbol{g}$	acceleration due to gravity ($9.8\,m\,s^{-2}$)
h	segment length (m)
I	mass moment of inertia ($kg\,m^2$)
l	leg length (m)
m	mass (kg)
SL	stride length (m)
SMR	standing metabolic rate ($W\,kg^{-1}$)
ST	stature (m)
t	time (s or percentage of the stride cycle)
TMR	treadmill metabolic rate ($W\,kg^{-1}$)
u	horizontal translational velocity ($m\,s^{-1}$)
v	translational velocity ($m\,s^{-1}$)
$\dot{V}_{O_2}$	volumetric rate of oxygen consumption
W	work ($W\,kg^{-1}$)
$\dot{W}$	experimentally determined mechanical power from the literature ($W\,kg^{-1}$)
x	distance along the x axis (m)
y	distance along the y axis (m)
z	distance along the z axis (m)
η	mechanical efficiency
θ	angular excursion (degrees)
ω	angular velocity ($rad\,\%^{-1}$ stride cycle or $rad\,s^{-1}$)

List of subscripts

ad	right calf
ae	right foot
bc	right half of pelvis
c	center of pelvis
cf	left half of pelvis
db	right thigh
ext	external
fg	left thigh
f	forward
gh	left calf
hi	left foot
i	current temporal increment
int	internal
i–1	previous temporal increment
k	kinetic
l	left leg
max	for a step
mod	modern human
p	potential
pe	pelvis
r	right leg
rl	right and left legs
std	standing plus control and balance
sum	summed value
tot	total
xx	about the x axis
xy	in the xy plane
xz	in the xz plane
yy	about the y axis
yz	in the yz plane

I wish to thank Dr Gerald G. Eck for his invaluable assistance with and support for this research. I am also greatly indebted to two anonymous reviewers for many helpful suggestions and criticisms of earlier versions of this work. In addition, I wish to thank Mr Brian J. Kramer for many hours of discussion of the dynamic principles upon which this effort is based.

References

Alexander, R. McN. (1984). Stride length and speed for adults, children and fossil hominids. *Am. J. Phys. Anthropol.* **63**, 23–27.

Cavagna, G. A., Heglund, N. C. and Taylor, C. R. (1977). Mechanical work in terrestrial locomotion, two basic mechanisms for minimizing energy expenditure. *Am. J. Physiol.* **233**, R243–R261.

Cavagna, G. A. and Kaneko, M. (1977). Mechanical work and efficiency in level walking and running. *J. Physiol., Lond.* **268**, 467–481.

Cavagna, G. A., Thys, H. and Zamboni, A. (1976). The sources of external work in level walking and running. *J. Physiol., Lond.* **262**, 639–657.

Chandler, R. F., Clauser, H. E., McConville, J. T., Reynolds, H. M. and Young, J. W. (1975). Investigation of inertial properties of the human body. DOT HS-801 430 (AMRL-TR-74-137). Washington, DC: US DOT.

Drake, R. and Curtis, G. H. (1987). Geology, dating and palynology K-Ar Geochronology of the Laetoli fossil localities. In *Laetoli A Pliocene Site in Northern Tanzania* (ed. M. D. Leakey and J. Harris), pp. 48–52. Oxford, UK: Clarendon Press.

FAO/UNU/WHO (1985). *Energy and Protein Requirements.* Technical Report Series No. 274. Geneva: World Health Organization.

Foley, R. A. (1992). Evolutionary ecology of fossil hominids. In *Evolutionary Ecology and Human Behavior* (ed. E. A. Smith and B. Winterhalder), pp. 131–164. New York: Aldine de Guyter.

Grieve, D. W. and Gear, R. J. (1966). The relationship between length of stride, step frequency, time of swing and speed of walking for children and adults. *Ergonom.* **5**, 379–399.

Inman, V. T., Ralson, H. J. and Todd, F. (1981). *Human Walking.* Baltimore, MD: Williams & Wilkins.

Jablonski, N. G. and Chaplin, G. (1993). Origin of habitual terrestrial bipedalism in the ancestor of the *Hominidae. J. Human Evol.* **24**, 259–280.

Johanson, D. C., Lovejoy, C. O., Kimbel, W. H., White, T. D., Ward, S. C., Bush, M. B., Latimer, B. L. and Coppens, Y. (1982). Morphology of the Pliocene partial hominid skeleton (AL 288-1) from the Hadar formation, Ethiopia. *Am. J. Phys. Anthropol.* **57**, 403–451.

Jungers, W. L. (1982). Lucy's limbs, skeletal allometry and locomotion in *Australopithecus afarensis*. *Nature* **297**, 676–678.

Jungers, W. L. (1991). A pygmy perspective on body size and shape in *Australopithecus afarensis* (AL 288-1, 'Lucy'). In *Origines de la Bipedie chez les Hominides* (ed. Y. Coppens and B. Senut), pp. 215–224. Paris, France: Editions du Centre National de la Recherche Scientifique.

Kramer, P. A. (1998). Locomotor energetics and limb length in hominid bipedality. PhD thesis, University of Washington, Seattle, WA, USA.

Latimer, B. and Lovejoy, C. O. (1989). The calcaneous of *Australopithecus afarensis* and its implications for the evolution of bipedality. *Am. J. Phys. Anthropol.* **78**, 369–386.

Latimer, B., Ohman, J. C. and Lovejoy, C. O. (1987). Talocrural joint in African hominoids, implications for *Australopithecus afarensis*. *Am. J. Phys. Anthropol.* **74**, 155–175.

Leakey, M. D. (1987). The hominid footprints. Introduction. In *Laetoli A Pliocene Site in Northern Tanzania* (ed. M. D. Leakey and J. Harris), pp. 490–495. Oxford, UK: Clarendon Press.

Leonard, W. R. and Robertson, M. L. (1992). Nutritional requirements and human evolution: A bioenergetics model. *Am. J. Human Biol.* **4**, 179–195.

Leonard, W. R. and Robertson, M. L. (1997). Comparative primate energetics and hominid evolution. *Am. J. Phys. Anthropol.* **102**, 265–281.

Lovejoy, C. O. (1988). Evolution of human walking. *Scient. Am.* **November** 118–125.

Lovejoy, C. O., Heiple, K. G. and Burnstein, A. H. (1973). The gait of *Australopithecus*. *Am. J. Phys. Anthropol.* **38**, 757–780.

McHenry, H. M. (1975). The ischium and hip extensor mechanism in human evolution. *Am. J. Phys. Anthropol.* **43**, 39–46.

McHenry, H. M. (1991a). Femoral lengths and stature in Plio-Pleistocene hominids. *Am. J. Phys. Anthropol.* **85**, 149–158.

McHenry, H. M. (1991b). First steps? Analysis of the postcranium of early hominids. In *Origines de la Bipedie chez les Hominides* (ed. Y. Coppens and B. Senut), pp. 133–141. Paris, France: Editions du Centre National de la Recherche Scientifique.

Meriam, J. L. (1978). *Dynamics*. New York: John Wiley & Sons, Inc.

NASA (1978). *Anthropometric Source Book.* Houston, TX: NASA Publication No. 1024.

Norkin, C. C. and Levangie, P. K. (1992). *Joint Structure and Function, A Comprehensive Analysis*. Philadelphia, PA: F. A. Davis Company.

Pandolf, K. B., Givoni, B. and Goldman, R. F. (1977). Predicting energy expenditure with loads while standing or walking very slowly. *J. Appl. Physiol.* **43**, 577–581.

Perry, J. (1992). *Gait Analysis Normal and Pathological Function.* Thorofare, NJ: Slack Inc.

Robbins, L. M. (1987). Hominid footprints from site G. In *Laetoli A Pliocene Site in Northern Tanzania* (ed. M. D. Leakey and J. Harris), pp. 496–502. Oxford, UK: Clarendon Press.

Robinson, J. T. (1972). *Early Hominid Posture and Locomotion.* Chicago, IL: University of Chicago Press.

Rodman, P. S. and McHenry, H. M. (1980). Bioenergetics and the origin of hominid bipedalism. *Am. J. Phys. Anthropol.* **52**, 103–106.

Stern, J. T. and Susman, R. L. (1983). The locomotor anatomy of *Australopithecus afarensis*. *Am. J. Phys. Anthropol.* **60**, 279–317.

Steudel, K. (1994). Locomotor energetics and hominid evolution. *Evol. Anthropol.* **3**, 42–48.

Tuttle, R. H. (1987). Kinesiological inferences and evolutionary implications from Laetoli bipedal trails G-1, G-2/3 and A. In *Laetoli A Pliocene Site in Northern Tanzania* (ed. M. D. Leakey and J. Harris), pp. 503–523. Oxford, UK: Clarendon Press.

Waters, R. L., Lunsford, B. R., Perry, J. and Byrd, R. (1988). Energy-speed relationship of walking, standard tables. *J. Orthop. Res.* **6**, 215–222.

Waters, R. L., Morris, J. and Perry, J. (1973). Translational motion of the head and trunk during normal walking. *J. Biomech.* **6**, 167–172.

Webb, D. (1996). Maximum walking speed and lower limb length in hominids. *Am. J. Phys. Anthropol.* **101**, 515–525.

Wheeler, P. E. (1991a). Thermoregulatory advantages of hominid bipedalism in open equatorial environments, the contribution of increased convective heat loss and cutaneous evaporative cooling. *J. Human Evol.* **21**, 107–115.

Wheeler, P. E. (1991b). Influence of bipedalism on the energy and water budget of early hominids. *J. Human Evol.* **21**, 117–136.

White, T. D. (1977). New fossil hominids from Laetoli, Tanzania. *Am. J. Phys. Anthropol.* **46**, 197–229.

White, T. D. (1980). Additional hominid fossils from Laetoli, Tanzania. *Am. J. Phys. Anthropol.* **53**, 487–504.

Willems, P. A., Cavagna, G. A. and Heglund, N. C. (1995). External, internal and total work in human locomotion. *J. Exp. Biol.* **198**, 379–393.

Williams, K. R. (1985). The relationship between mechanical and physiological energy estimates. *Med. Sci. Sports Exerc.* **17**, 317–325.

Winter, D. A. (1987). *The Biomechanics and Motor Control of Human Gait.* Waterloo, Ontario, Canada: University of Waterloo Press.

Witte, H., Recknagel, S. and Preuschoft, H. (1991). Human body proportions explained on the basis of biomechanical principles. *Z. Morph. Anthropol.* **78**, 407–423.

Zihlman, A. L. (1978). Interpretations of early hominid locomotion. In *Early Hominids of Africa* (ed. C. J. Jolly), pp. 361–377. London, UK: Duckworth.

Zihlman, A. L. (1984). Body mass and tissue composition in *Pan paniscus* and *Pan troglodytes*, with comparisons to other hominoids. In *The Pygmy Chimpanzee Evolutionary Biology and Behavior* (ed. R. Susman), pp. 179–200. New York, NY: Plenum Press.

Zihlman, A. L. and Brunker, L. (1979). Hominid bipedalism then and now. *Yearbook Phys. Anthropol.* **22**, 132–162.